

High vertical resolution measurements of pH, pCO₂, total alkalinity, and dissolved inorganic carbon using a new approach: the carbonate profiler

Fernando Aguado Gonzalo, Katarzyna Koziorowska, Laura Bromboszcz-Szczypior, Alexandra Loginova, Karol Kuliński

Abstract

The equilibrium between the different parameters of the marine carbonate system – dissolved inorganic carbon (DIC), total alkalinity (TA), partial pressure of CO₂, and pH – is the core of ocean acidification studies, evaluation of inorganic carbon inventory, and air-sea CO₂ fluxes. To date, it has been challenging to simultaneously measure all those components in the water column due to different sampling methodologies, and especially in stratified waters, where sharp vertical biogeochemical gradients may occur. In this study, we designed a low-cost and easy-to-assemble pumping system, which, combined with a CTD profiler, makes a PUMP-CTD system that can efficiently serve as a precise water column sampler, allowing for simultaneous measurements and sampling of dissolved inorganic carbon, total alkalinity, partial pressure of CO₂, and pH with high vertical resolution. Importantly, this water sampler (denoted as the carbonate profiler) can be easily integrated with equilibrator-based continuous pCO₂ measurement systems, which are routinely used for underway data acquisition, making them suitable for water column sampling as well. We tested the carbonate profiler in the open ocean water column, where we obtained excellent consistency between measured pCO₂ and calculated values based on pH and DIC. Afterwards, we tested the operability of the system by measuring the vertical variability of all the components of the marine carbonate system in the Vistula River estuarine waters (southern Baltic Sea) and within the Arctic fjords affected by continental freshwater runoff. Overall, this system performed outstandingly, with a vertical resolution of half a meter, proving its utility in accurately measuring steep biogeochemical changes in the water column regardless of the analytical method used.

Keywords

Ocean acidification; pH; Total alkalinity; pCO₂; Land ocean continuum; Arctic; Baltic Sea

Institute of Oceanology, Polish Academy of Sciences, Powstańców Warszawy 55, 81-712 Sopot, Poland

*Correspondence: aguadof@iopan.pl (F. Aguado Gonzalo)

Received: 26 June 2025; revised: 4 November 2025; accepted: 12 November 2025

1. Introduction

The Oceans are key components for mitigating climate change due to their capacity to absorb atmospheric carbon dioxide (CO₂) at the surface and export it to the deeper water layers and sediments (Friedlingstein et al., 2025). Among oceanic regions, coastal areas, which often have very high carbon fixation rates, are key contributors to carbon export driven by intense primary production (Cai, 2011). As such, they are vital components of the global carbon cycling (Bauer et al., 2013; Dai et al., 2022; Regnier et al., 2022). However, the total contribution of these regions to the global carbon budget remains uncertain due to high spatiotemporal

biogeochemical variability (Cai, 2011; Resplandy et al., 2018).

Within the coastal areas, estuaries represent complex biogeochemical environments where particulate and dissolved organic and inorganic carbon compounds of both autochthonous and allochthonous origin undergo rapid transformations (Mosley and Liss, 2020). In addition to commonly investigated processes related to organic matter production and remineralization (sink and source of CO₂, respectively), including respiration of terrigenous organic matter (Cross et al., 2018; Kuliński et al., 2016), carbon transformations are also driven here by significant shifts in pH and ionic composition resulting from the mixing of freshwater and seawater. In turn, pH, or concentration of protons (pH = $-\log[H]$), is mainly controlled

29 by the excess of proton acceptors over proton donors in
30 water, defined as total alkalinity (TA) (Dickson, 1981). In
31 the compounds that make up TA, the largest share comes
32 from two inorganic carbon species, namely bicarbonate
33 (HCO_3^-) and carbonate (CO_3^{2-}) ions, which together with
34 dissolved CO_2 (or H_2CO_3) constitute dissolved inorganic
35 carbon (DIC). Therefore, there is an intricate balance be-
36 between pH, TA, and DIC, which ultimately determines dis-
37 solved CO_2 concentrations expressed most often as CO_2
38 partial pressure (pCO_2) (e.g., Millero, 2007). These four
39 measurable parameters and their chemical interactions
40 are often referred to as the marine carbonate system. Bio-
41 logical, physical and chemical processes continuously alter
42 the delicate equilibrium between these parameters, initiating
43 cascade changes in all of them. Therefore, to estimate
44 the effect of biogeochemical processes and air-sea CO_2 ex-
45 change on the carbon inventory and fluxes in the coastal
46 areas, it is necessary to characterize the complex horizontal
47 and vertical distribution of all the marine carbonate
48 system parameters.

49 While the variables of the marine carbonate system are
50 interrelated, their measurement approaches differ. Gener-
51 ally, pCO_2 is obtained using the well-established underway
52 systems, in which continuously flowing water is equili-
53 brated with a closed air loop where pCO_2 is measured.
54 These systems can provide highly accurate data with un-
55 certainties lower than 2 μ atm or 0.5% of the measured
56 values (e.g., Arruda et al., 2020; Stokowski et al., 2021a).
57 However, they are designed and installed on research ves-
58 sels and ships of opportunity to obtain measurements at
59 a fixed depth corresponding to the water inlet depth of the
60 vessel's pumping system (typically between 2 and 10 m
61 water depth). This setup makes them suitable for studying
62 the horizontal distribution of pCO_2 but inappropriate for
63 resolving vertical gradients in the water column. Although
64 they are being used to estimate air-sea CO_2 fluxes in ar-
65 eas where sharp vertical gradients of CO_2 are expected, it
66 has been demonstrated that differences in the sampling
67 depth can introduce significant errors in the results (e.g.,
68 Ahmed et al., 2020; Azevedo et al., 2024). Thus, capturing
69 the vertical distribution of pCO_2 in the water column is
70 essential for precise flux calculations in stratified waters.
71 Recent advances in underwater CO_2 sensors enable in situ
72 measurements of CO_2 in the entire water column (when
73 mounted on CTD profilers) or at a fixed depth for extended
74 monitoring (when deployed in mooring systems). How-
75 ever, they often have lower accuracy and longer response
76 times (between 5 and 20 minutes) than underway sys-
77 tems (Arruda et al., 2020; Clarke et al., 2017; Schar et al.,
78 2010b).

79 Similarly, high vertical resolution TA, DIC, and pH
80 measurements are challenging due to sampling
81 limitations. Water for these analyses is commonly col-
82 lected using bathometers, typically mounted in sampling
83 carousels with a vertical resolution not better than 2–3 m,

84 which is often insufficient to study rapid biogeochemi-
85 cal gradients in the water column. Moreover, the num-
86 ber of samples collected in the profile is directly corre-
87 lated with the number of Niskin bottles mounted in the
88 sampling carousel, which significantly limits the resolu-
89 tion of the sampling. For pH, direct measurements in the
90 water column are also possible using submersible sen-
91 sors. Several can perform spectrophotometric measure-
92 ments directly in the water column, providing high-quality
93 data (Bresnahan et al., 2014; Johengen et al., 2015). How-
94 ever, their response time (5–15 minutes) is usually too
95 slow to obtain water column pH profiles with high vertical
96 resolution.

97 In addition to direct measurements, each of the two
98 marine carbonate variables can be calculated from the
99 other two, which are known from direct measurements or
100 modelling. This requires the use of thermodynamic ion-
101 pairing models describing the carbonate system (Lewis et
102 al., 1998). However, these models are primarily dedicated
103 to open ocean waters where the marine carbonate system
104 is well characterized. Their application in coastal areas
105 remains challenging (Aguado Gonzalo et al., 2025a) due
106 to anomalies in seawater composition and the influence
107 of non-parameterized seawater constituents, leading to
108 significant errors in calculations (Kerr et al., 2023; Kuliński
109 et al., 2017; Ulfsbo et al., 2015). Thus, to characterize the
110 marine carbonate system in coastal regions, it is often nec-
111 essary to measure the complete set of variables (pCO_2 ,
112 TA, DIC, and pH). This approach can be considered exces-
113 sive or redundant in ocean waters. Such comprehensive
114 sampling, especially in stratified waters, requires careful
115 planning, standardization of the vertical resolution, and
116 unification of the sampling technique for all parameters,
117 regardless of the analytical methods used later. This is
118 particularly important for combining state-of-the-art high-
119 quality methods based on collecting discrete samples (TA,
120 DIC, pH) with pCO_2 measurements, which require contin-
121 uous water flow through the equilibrator (Dickson et al.,
122 2007).

123 These challenges were the motivation to undertake
124 this study, the aim of which was to design a sampling
125 system that: (i) is capable of simultaneous discrete
126 sampling of TA, DIC and pH and continuous equili-
127 brator-based pCO_2 measurements in a vertical profile, (ii)
128 allows easy switching in water supply between on-station
129 vertical profiling and underway mode, (iii) inexpensive
130 and easy to implement on a variety of vessels, including
131 small ones, and (iv) provides high-quality results describ-
132 ing the marine carbonate system. The latter has been
133 proven by tests made in the open waters of the Green-
134 land Sea, while the operability of the system has been
135 tested in two different coastal environments: the turbid
136 freshwater plumes in the high Arctic fjords and the mid-
137 latitude estuarine system of the Vistula River in the Baltic
138 Sea.

2. Material and methods

2.1 The carbonate profiler

The inspiration for the system setup was a PUMP-CTD concept as reported, for instance, by Strady et al. (2008). However, the PUMP-CTD we designed was coupled with an equilibrator-based pCO_2 measurement system typically used for underway sampling. Thus, this carbonate profiler follows a similar principle as any underway system for pCO_2 measurements: a pump carries water along a pipeline to the ship's laboratory, where it flows continuously through the equilibrator whose headspace is connected by a closed air loop to a CO_2 analyser, while an additional water bypass allows for discrete sampling for TA, DIC, pH or any other parameter. The sole distinction of the carbonate profiler is the water supply, which is a submersible pump attached to the CTD profiler and deployed together with it by a winch. The pump provides water from a desired depth in the water column using a flexible and retractable plumbing system, which is deployed simultaneously with the CTD cable. In this study, we developed a system capable of sampling water from a maximum depth of 60 m, which is generally sufficient to investigate the variability of the carbonate system in both the mixing zone and the photic zone. A simplified scheme of the system installed in r/v *Oceania* is presented in Figure 1.

Our ambition was to develop a system that is inexpensive, transportable, and easy to implement on a variety of vessels, including smaller ones. The latter requires that the system can interoperate with any CTD profiler the vessel is equipped with. In our case, it was a Sea-Bird 19plus

(Sea-Bird Electronics, Inc., Bellevue, Washington, USA) to which the submersible pump was attached, ensuring that the water inlets to both units were at the same depth to unify CTD readings with carbonate chemistry measurements. The submersible pump used in this prototype was a Pedrollo 3SR2/28 (www.pedrollo.com, San Bonitacio, Italy), with a deployment depth of approximately 60 m and an adjustable flow rate (through the power controller) between 10–50 L min⁻¹ that may further depend on how high the water needs to be pumped above the ocean surface. This high water flow minimized the transport time to the laboratories and greatly exceeded the flow required for continuous pCO_2 measurements (approximately 0.8 L min⁻¹); therefore, excess water was bypassed, allowing for sampling of TA, DIC, and pH, as well as additional in-lab CTD measurements. All the pipes in the system had the same diameter, and narrow pipe connectors were avoided to elude overpressure. The flexible pipe system consisted of a commercially available Gardena Classic 3/4" PVC cross-woven fabric hose (Gardena, www.gardena.com, Ulm, Germany), directly connecting the submersible pump to the ship's laboratories. The delay time, which is necessary for sampled water to be transported to laboratories, depends on the length of the hose deployed and the water flow. In our case, it was 19.5 seconds, calculated for a pipe length of 120 m and a water flow rate of 40 L min⁻¹. To minimise temperature changes during sampling, the hose system was not placed under direct sunlight or on warm surfaces. In the laboratories, four T-connectors equipped with flow regulators were installed to split the water flow to: (i) the equilibrator-based continuously measuring pCO_2 sys-

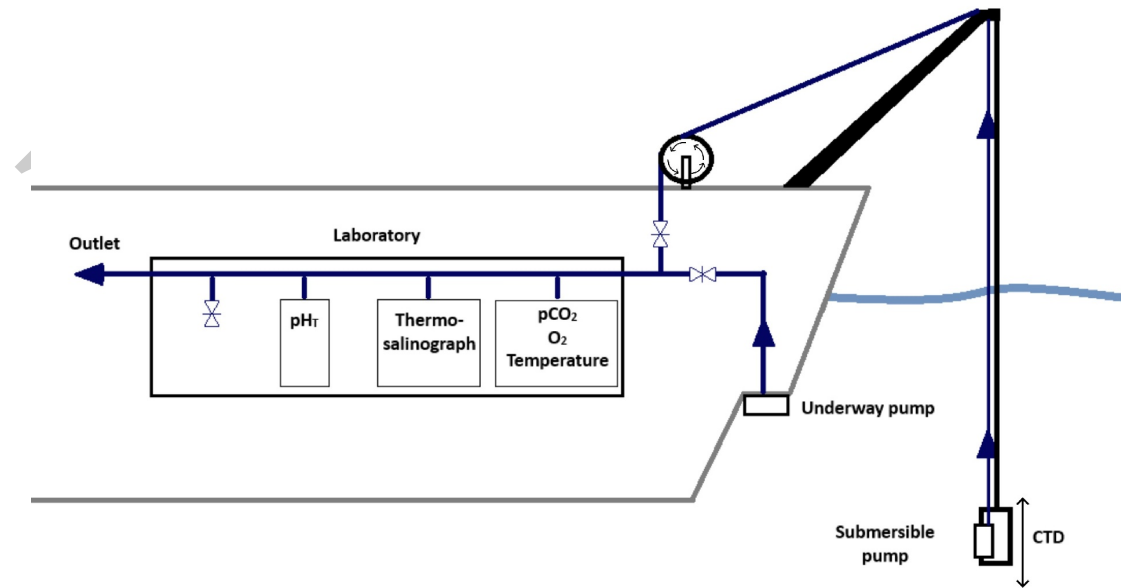


Figure 1. Simplified schematic representation of the carbonate profiler for a semi-continuous, precise sampling of the marine carbonate parameters in the water column.

tem, (ii) the flow-through thermostalinograph, (iii) the pH-spectrophotometer unit, and (iv) free-flowing water for collecting discrete samples for different analyses, in our case, DIC, TA, and in some cases also pH. Furthermore, additional valves enable immediate switching of the water source between the submersible PUMP-CTD and the ship's underway pumping system (having a water inlet at a fixed depth, 2.5 m on *r/v Oceania*), allowing the same laboratory equipment to be used for horizontal and vertical measurements (Figure 1). Importantly, the entire system consists of only quick connectors, making it easy to install, uninstall, and transport.

2.2 The laboratory instrumentation and analytical techniques

Measurements of pCO_2 were carried out using the system described in detail by Stokowski et al. (2021a). The system consists of a bubble-type equilibrator where the seawater flowing in is additionally sprayed using a shower diffuser. The air from the headspace flows along a closed loop through a cavity ring-down spectrometer (CRDS) G2101-I (Picarro). The quality of the measurements was regularly monitored using three gases with different CO_2 concentrations: 0, 205, and 507 ppm, which enabled achieving an accuracy and precision of $\pm 1.3 \mu\text{atm}$. The effect of temperature changes during water transport from the PUMP-CTD to the laboratory has been corrected using the function proposed by Takahashi et al. (1993) (Eq. 1), so that the pCO_2 measured in the equilibrator, $pCO_2(\text{lab})$, was recalculated to the in situ temperature, $pCO_2(\text{in situ})$.

$$pCO_2(\text{in situ}) = \quad (1)$$

$$pCO_2(\text{lab}) \times \exp(0.0423 \times (t_{(\text{in situ})} - t_{(\text{lab})}))$$

All pCO_2 measurements were also standardized to 1 atmosphere of pressure to remove the effect of atmospheric pressure changes in the final results, using Equation 2.

$$pCO_2(1\text{ atm}) = pCO_2(\text{in situ}) \times 1012.25/P \quad (2)$$

The pH measurements were carried out on board using a HydroFIA flow-through spectrophotometric system (CONTROS, 4H-JENA engineering GmbH), directly connected to the carbonate profiler plumbing system. The pH was estimated spectrophotometrically using mCresolPurple as an indicator agent (Carter et al., 2013; Clayton and Byrne, 1993; Liu et al., 2015; Mosley et al., 2004). The accuracy of the pH measurements was ensured by routine measurements of TRIS-buffer (TRIS-CRM-T37) provided by A.G. Dickson (Scripps Institution of Oceanography, USA), which showed an accuracy/precision better than ± 0.003 . All pH measurements were performed at 25°C, and the results were reported on the total scale.

The discrete water samples for analysis of TA and DIC were collected in 270 mL borosilicate glass bottles using the free-flowing bypassed water from the carbonate profiler. Samples were carefully poured from the bottom of the bottle to avoid air bubbles and left overflowing for at least 10 seconds. Next, 1 mL of the sample was removed to allow thermal expansion, and 100 μL of saturated $HgCl_2$ was added to inhibit/prevent biological activity. All the bottles were closed with greased ground-glass stoppers and stored in the dark at +4°C until analysis.

The TA was estimated using the methodology described in Dickson et al. (2003). Open cell titrations were carried out using a Methrom 888 Titrando, equipped with a 1mL burette. Total alkalinity was calculated from the potentiometric titration curves using version V23 of the Python package "Calkulate" (Humphreys and Matthews, 2024). The accuracy of the measurements was estimated by repeated measurements of Certified Reference Material (CRM) batch #CRM-209, provided by A.G. Dickson (Scripps Institution of Oceanography, USA). At least three measurements of CRM were done before and after the batch of samples until a precision better than $\pm 2 \mu\text{mol kg}^{-1}$ was achieved. Any deviation from the CRM values was corrected accordingly, and the accuracy correction was applied to a batch of samples. Each sample was measured in triplicate with a precision always better than $\pm 3 \mu\text{mol kg}^{-1}$. The same methodology was applied to all samples. However, some were analyzed on board and others in the laboratories of the Institute of Oceanology, Polish Academy of Sciences (IO PAN), within a maximum time of four weeks.

The concentration of DIC was determined using an automated DIC analyzer (Apollo SciTech Inc.), equipped with a Li7815 CO_2 detector and following the methods described by Chen et al. (2015). All the measured samples were cross-calibrated with measurements of the CRMs (same as for TA), assuring an accuracy of $\pm 2 \mu\text{mol kg}^{-1}$ during the sample measurements. Each sample and CRM was measured at least three times until a precision better than $\pm 1.5 \mu\text{mol kg}^{-1}$ was achieved. All the measurements were carried out in the IO PAN laboratories within a maximum of four weeks after collection.

2.3 Calculations of the carbonate system parameters

Calculations of pCO_2 and estimations of the uncertainties related to the calculated values were carried out using the Excel version of the CO_2 sys program (Pierrot et al., 2006), as published by Orr et al. (2018). For the calculations, the carbonic acid dissociation constants (K1 and K2) from Lueker et al. (2000) were used together with the $KHSO_4$ from Dickson et al. (1990), the fluoride dissociation constant of Perez and Fraga (1987), and the boron to chlorinity ratio of Lee et al. (2010). All calculations were reported to 1 atmosphere to minimize errors due to recalculations to in situ pressure. The uncertainties related to the dissociation constants and the K1/K2 ratio were set to 0.001.

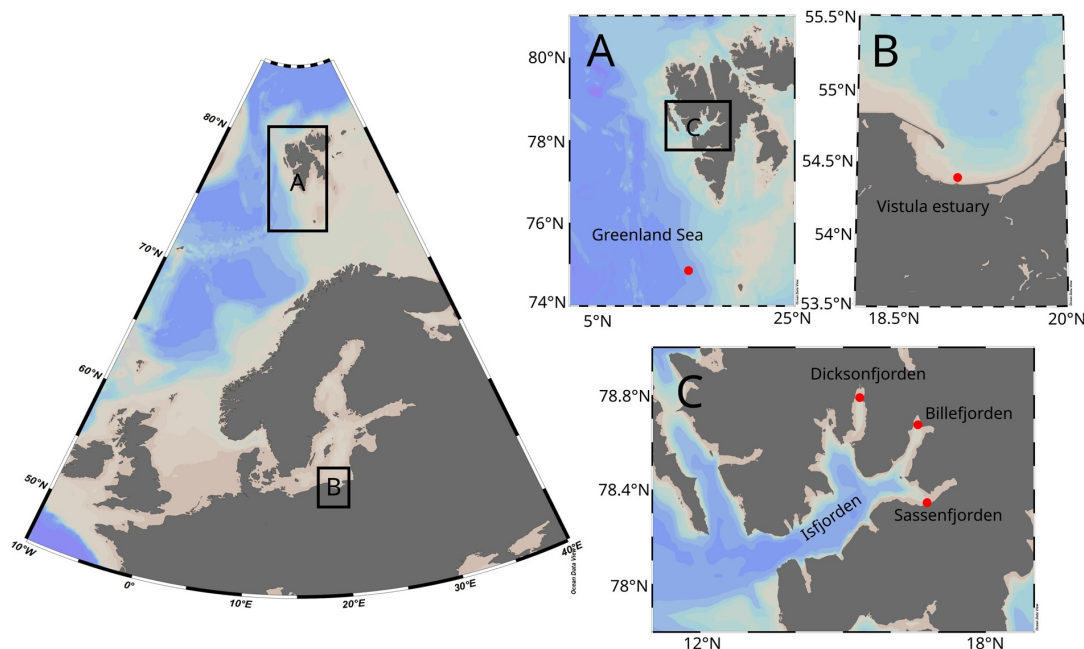


Figure 2. Location of the sampling stations (red dots). A) Greenland Sea. B) Baltic Sea. C) Svalbard fjords.

tion constants used in this study were extracted from Orr et al. (2018).

2.4 Sampling strategy and study area

For this study, sampling was conducted in three different areas, resulting in a total of eight water column profiles collected. Two study areas were located in stratified coastal systems (the Svalbard archipelago and the southern Baltic Sea), and one was located in the open waters of the Greenland Sea (Figure 2). The open ocean profile was sampled in July 2024 ($74^{\circ}59'58.2''N$; $13^{\circ}10'56.9''E$), away from continental waters, where the marine CO_2 system is well characterized and where good consistency between measured and calculated values was expected based on previous studies (Aguado Gonzalo et al., 2024). These features enabled us to evaluate the sampling system's ability to simultaneously obtain thermodynamically coherent results for pCO_2 , TA, and pH in the water column and verify the quality of the measured pCO_2 by comparing it with the pCO_2 calculated from TA and pH measurements.

In the coastal areas, the tests of the carbonate profiler have been performed in regions known for their highly stratified waters with sharp biogeochemical gradients. These sampling areas enabled us to evaluate the operability and capability of the carbonate profiler in resolving complex vertical variability. Four profiles were collected during spring 2024 within the Vistula River estuary ($54^{\circ}22'40.8''N$; $18^{\circ}55'30.0''E$), located in the southern Baltic Sea (Figure 2). This region is characterized by the influence of TA-rich river waters and large gradients in the carbonate system parameters caused by the changing extent of the river plume and thus variable water strati-

fication (Stokowski et al., 2021b). All four profiles were taken in the same location, but at six-hour intervals. The reason for that was to estimate the short-term variability of the carbonate system in the region and assess the reproducibility of the freshwater TA end member from the extrapolated dependency against salinity, which should be relatively conservative in such a short time period.

Additionally, three more profiles were obtained in August 2022 in the high Arctic fjords within the Svalbard archipelago (Figure 2). The sampling locations were selected in areas with a strong influence of freshwater turbid plumes. These plumes are produced by continental runoff, mainly fed by meltwater from land-terminating glaciers, and abrupt biogeochemical gradients are expected within the first 10 meters of the water column (e.g., Meslard et al., 2018; Szeligowska et al., 2020).

3. Results and discussion

3.1 Estimated quality of the carbonate profiler measurements

To demonstrate the system's capability to obtain accurate measurements of carbonate system variables in the water column, we compared measured and calculated (from pH and TA) values of pCO_2 in the oceanic waters of the Greenland Sea. These results, along with their uncertainties, are presented in Figure 3, which also shows the absolute differences between measured and calculated values, $\Delta pCO_2(\text{meas-calc})$. Our results indicate that the first five samples collected in the water column (down to a water depth of 40 m) exhibited small variability ($SD = \pm 3.6 \mu\text{atm}$) with an average measured pCO_2 of $308.8 \mu\text{atm}$. On

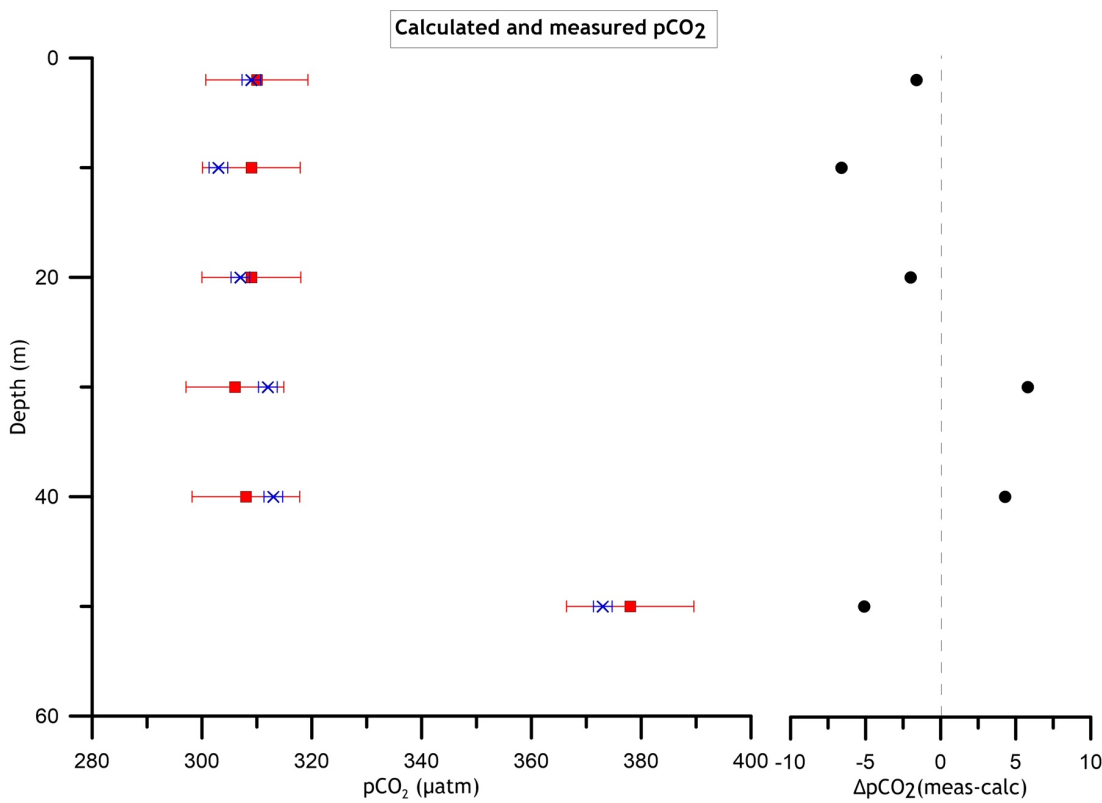


Figure 3. Left: measured (blue cross) and calculated (red square) pCO_2 . The error bars indicate the uncertainty in the measured/calculated values. Right: the absolute differences between pCO_2 measured and calculated out of TA and pH.

361 the other hand, at a water depth of 50 m, the pCO_2 was
 362 significantly higher, amounting to 373 μ atm, indicating
 363 a rapid increase of 64 μ atm (Figure 3). The abrupt pCO_2
 364 gradient between 50 and 60 m water depth was also suc-
 365 cessfully captured by TA and pH sampling, as indicated by
 366 the perfect agreement between the measured and calcu-
 367 lated pCO_2 values. Hence, the ΔpCO_2 (meas-calc) exhibited
 368 a low average of $\bar{x}(SD) = 0.9(\pm 4.5)$ μ atm, indicating an
 369 excellent performance of the carbonate profiler that en-
 370 ables consistent sampling of different carbonate system
 371 parameters despite differences in measurement method-
 372 ologies requiring either continuous water flow or discrete
 373 sampling.

374 A similar exercise, as presented here, but using only
 375 surface data, was presented by Carter et al. (2024). In
 376 their study, the authors collected state-of-the-art surface
 377 open-ocean pCO_2 , pH, and TA data from the Global Ocean
 378 Data Analysis Project 2022 update (GLODAPv2.2022) to
 379 estimate the (in)consistency between measured and cal-
 380 culated variables of the marine carbonate system. Their
 381 results show that the average of the relative difference be-
 382 tween measured and calculated (from TA and pH) fCO_2 (fu-
 383 gacity of CO_2) was 1.8% of the measured fCO_2 (equivalent
 384 to ± 5.6 μ atm for 308.8 μ atm). Following the calculation
 385 method described by Carter et al. (2024), we transferred
 386 our water column results to fCO_2 and presented them as

387 a percentage of the measured value. Our results indicated
 388 a relative difference of 1.4 (± 4.5 μ atm), which is a better
 389 agreement than the one previously reported. Similarly to
 390 the study by Carter et al. (2024), but restricted to Arctic
 391 Oceanic surface waters, Woosley et al. (2017) and Aguado
 392 Gonzalo et al. (2024) reported discrepancies between mea-
 393 sured and calculated pCO_2 of ± 5.3 and ± 5 μ atm, respec-
 394 tively, which are slightly worse than the ones reported here
 395 (± 4.5 μ atm). Furthermore, the real observed uncertainty
 396 of ± 4.5 μ atm for the difference between measured and
 397 calculated pCO_2 was significantly lower than the theoretical
 398 one (± 9 μ atm) derived from the propagation of all the
 399 initial uncertainties (see methods). This difference in the
 400 uncertainty suggests that any deviations in pCO_2 measured
 401 versus pCO_2 calculated, ΔpCO_2 (meas-calc), are solely due
 402 to uncertainties in the thermodynamic model of the ma-
 403 rine CO_2 system, while the carbonate profiler guarantees
 404 high-quality, continuous pCO_2 measurements that are per-
 405 fectly consistent with semi-continuous pH measurements
 406 and discrete sampling for TA.

407 This profile took about 25 minutes to complete in to-
 408 tal. This time was a result of sampling at each depth and
 409 the time required to move the system between sampling
 410 levels. The time needed to obtain a complete set of results
 411 from a given depth was estimated based on the response
 412 time of the pCO_2 equilibrator, which was previously mea-
 413 sured.

sured by Stokowski et al. (2021a), where the time to reach 63% of the equilibration (T63) was 68 seconds and an the effective equilibration time (T99) was 1 minute and 44 seconds (approx. 2 min). Thus, we maintained the PUMP-CTD for at least 3 minutes at each depth to ensure that measurements were taken after the equilibrium was reached. The excellent results from the consistency exercise demonstrated that this time was certainly sufficient to reach equilibrium. Based on calculations and earlier estimations by Stokowski et al. (2021a), we believe there is still room to optimize sampling time. Unfortunately, due to operational constraints of the open ocean cruise, no further tests were performed.

Nevertheless, the sampling time was satisfactorily short, especially since samples for additional parameters were taken in parallel. Commercially available submersible CO₂ sensors offer a range of response times and effective measurement intervals. However, all of them are slower than the carbonate profiler, which allows easy adaptation of underway surface pCO₂ measurement systems for water column sampling. For example, CO₂ sensors based on pH indicators (e.g., Sunburst sensors, SAMI-CO₂) have a response time of approximately 5 minutes (Lai et al., 2018). In comparison, sensors based on non-dispersive infrared (NDIR) gas analyzers equipped with hydrophobic equilibration membranes (e.g., Pro-Oceanus Systems Inc. PSI CO₂-ProTM, C-Sense pCO₂, CONTROS HydroC CO₂) have typical measurement intervals and equilibration times of 10 to 15 minutes (Fietzek et al., 2014; Jiang et al., 2014; Schar et al., 2010b; Signori et al., 2021).

In addition to the higher sampling speed, the carbonate profiler system presented here shows excellent pCO₂ measurement accuracy (reported above and by Stokowski et al. (2021a)), which is hardly achievable with submersible sensors. For instance, the SAMI-CO₂ sensor was able to collect data with an accuracy of $+40 \pm 13 \mu\text{atm}$ (x and SD) during a field test (Schar et al., 2010b). In the case of Pro-Oceanus Systems Inc. PSI CO₂-ProTM, a similar test reported a \bar{x} and SD of $+9 \pm 14 \mu\text{atm}$ (Schar et al., 2010a), while Fietzek et al. (2014) reported an x and SD of $-0.6 \pm 3.0 \mu\text{atm}$ using a CONTROS HydroC CO₂.

To sum up, the high-quality water column pCO₂ results obtained in this study, along with the rapid sampling, including the possibility of collecting other carbonate system parameters in parallel, demonstrate the excellent performance of the carbonate profiler we designed, which is currently unachievable for sensor-based measurements on research vessels.

3.2 Performance of the carbonate profiler in highly stratified waters

3.2.1 Test 1: The mid-latitude estuary system of the Vistula River plume

The variability of TA, DIC, pH, and pCO₂, as well as salinity and temperature observed in the first 10 meters of the

water column in the estuarine system of the Vistula River plume, is presented in Figure 4. In all the profiles, salinity and pCO₂ increased with depth, while pH, DIC, and TA decreased, indicating that the Vistula River water affecting this area had higher DIC, TA, and pH, and lower pCO₂. These results demonstrate that, thanks to the carbonate profiler, it was possible to resolve steep biogeochemical gradients, with ranges spanning up to 2050 $\mu\text{mol kg}^{-1}$ for TA, approximately 1700 $\mu\text{mol kg}^{-1}$ for DIC, 166 μatm for pCO₂, and 0.58 for pH, respectively. Herewith, DIC, TA and salinity were characterized by rapid changes within the first two meters of the water column and apparently varied among profiles, showing the spectrum of variability in riverine plume dynamics at a single location within the 24-hour sampling period. On the other hand, pCO₂ showed only slight changes within the first two meters, with comparable values between profiles (ranging from 217 to 246 μatm), suggesting strong primary production in the surface water layer, regardless of the scale of the Vistula River impact. Below this level, the pCO₂ increased significantly with depth, reaching values of up to 413 μatm at 10 m. Apart from being the first insight into the carbonate system structure in the water column of the region, these results clearly demonstrate the complexity and the vertical variability in stratified waters. Special attention should be paid to the vertical distribution of pCO₂, which highlights the importance of the sampling depth from which pCO₂ results are obtained for estimating air-sea CO₂ diffusive fluxes, a feature also discussed earlier by Ahmed et al. (2020) and Azevedo et al. (2024). Thus, underway pCO₂ measurements describing horizontal variability should always be combined with vertical profiling in stratified waters. For this, the carbonate profiler designed and described in this study provides an easy-to-use and low-cost solution that can significantly improve the estimation of air-sea CO₂ fluxes.

The relationship between TA and salinity exhibited a conservative behavior during sampling (Figure 5), with an excellent correlation ($R^2 = 0.98$). It demonstrates that the carbonate profiler attached to the CTD (PUMP-CTD) enabled the collection of water from a precise depth where salinity was measured, providing reliable vertical accuracy of sampling for carbonate system parameters. We took water samples at every half-meter interval in the first two meters of the water column and at every meter interval in the deeper water layer. This vertical resolution was sufficient to record the changes in the marine carbonate system parameters in the water column of this stratified area. However, the good correlation between salinity and TA suggests that even higher vertical resolution could be achieved. The freshwater TA end member estimated from the linear regression between salinity and TA collected for all four profiles amounted to 4069 $\mu\text{mol kg}^{-1}$ ($\text{SD}=12 \mu\text{mol kg}^{-1}$). This value exceeds the previously reported range for the Vistula River (from 3136 to 3746 $\mu\text{mol kg}^{-1}$) by Stokowski

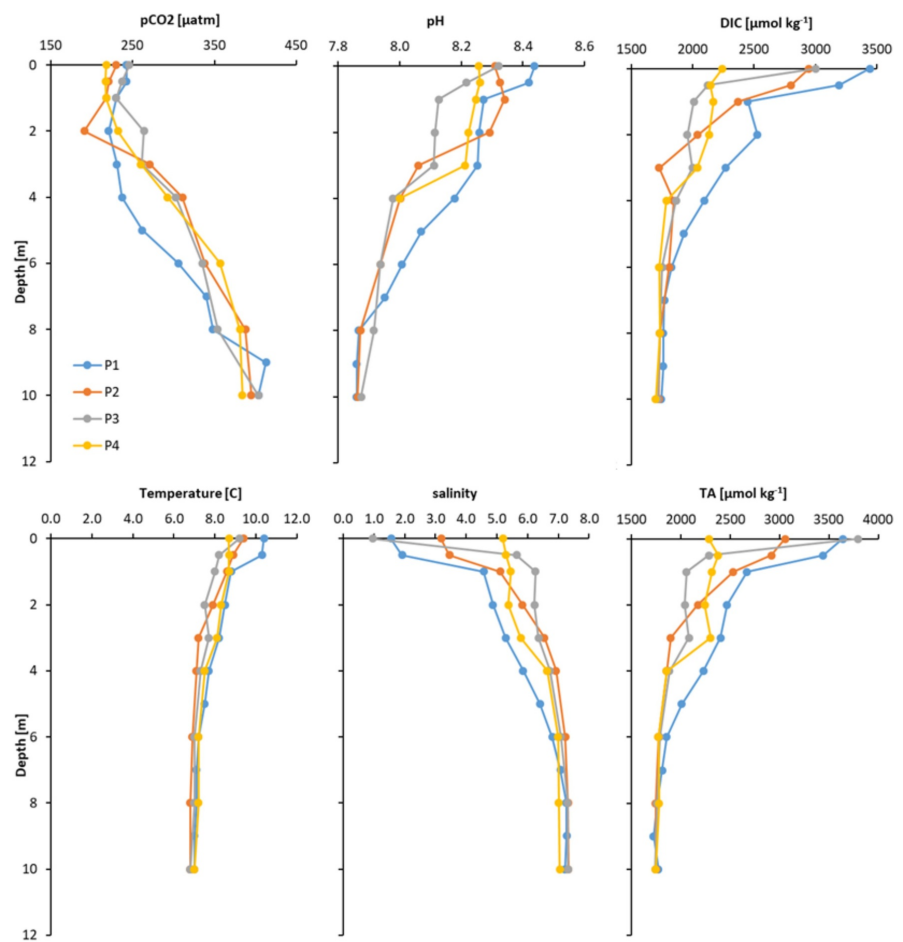


Figure 4. Vertical distribution of pCO_2 , pH, DIC, TA, temperature, and salinity during four samplings (P1–P4) performed in one spot in the Vistula River plume in 6-hour intervals.

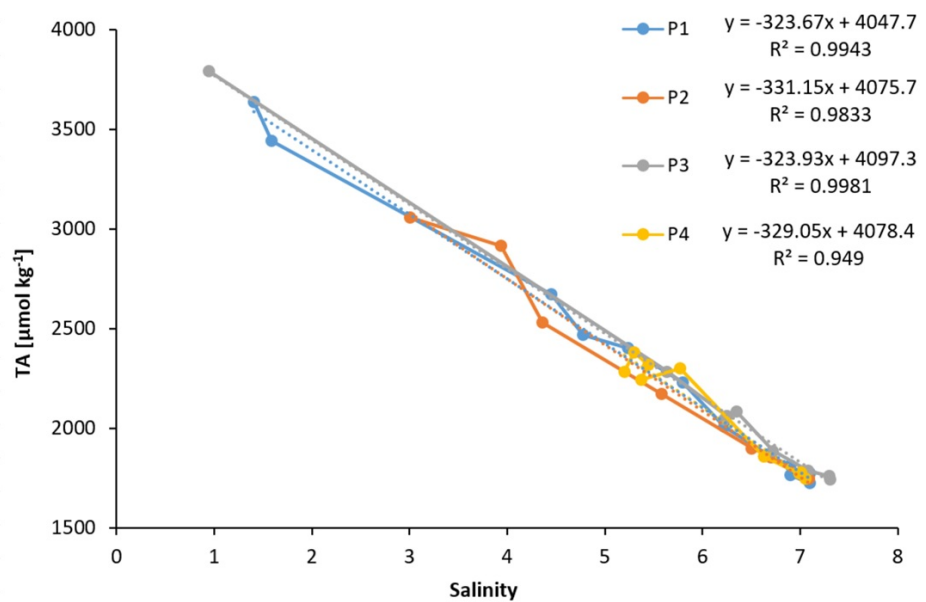


Figure 5. Linear correlation between salinity and TA during the four vertical profiles performed in one spot in the Vistula River plume at 6-hour intervals.

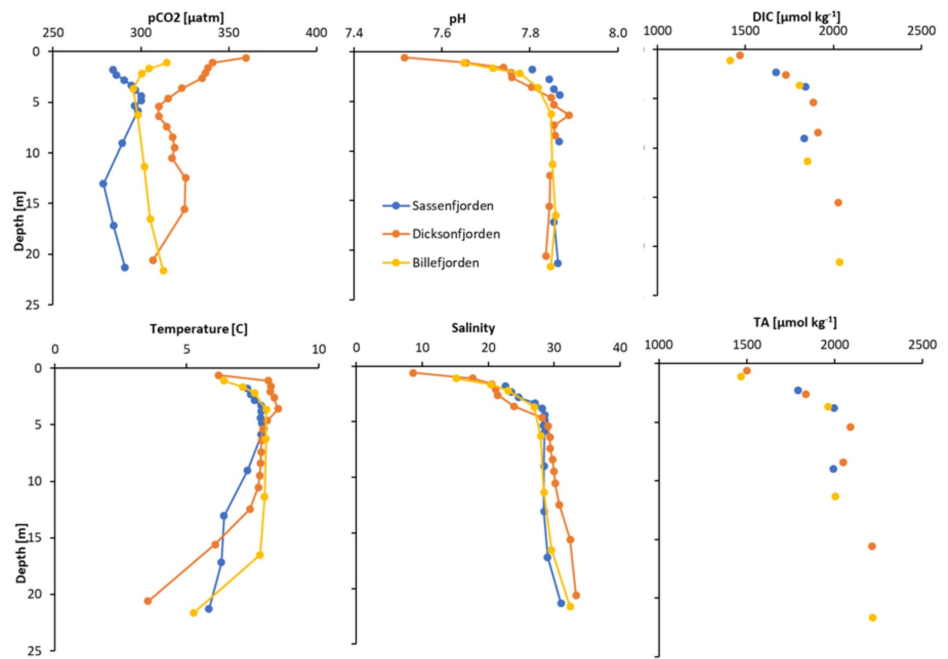


Figure 6. Vertical distribution of the marine carbonate system parameters (pCO₂, pH, DIC, TA), temperature, and salinity in the three Spitsbergen fjords.

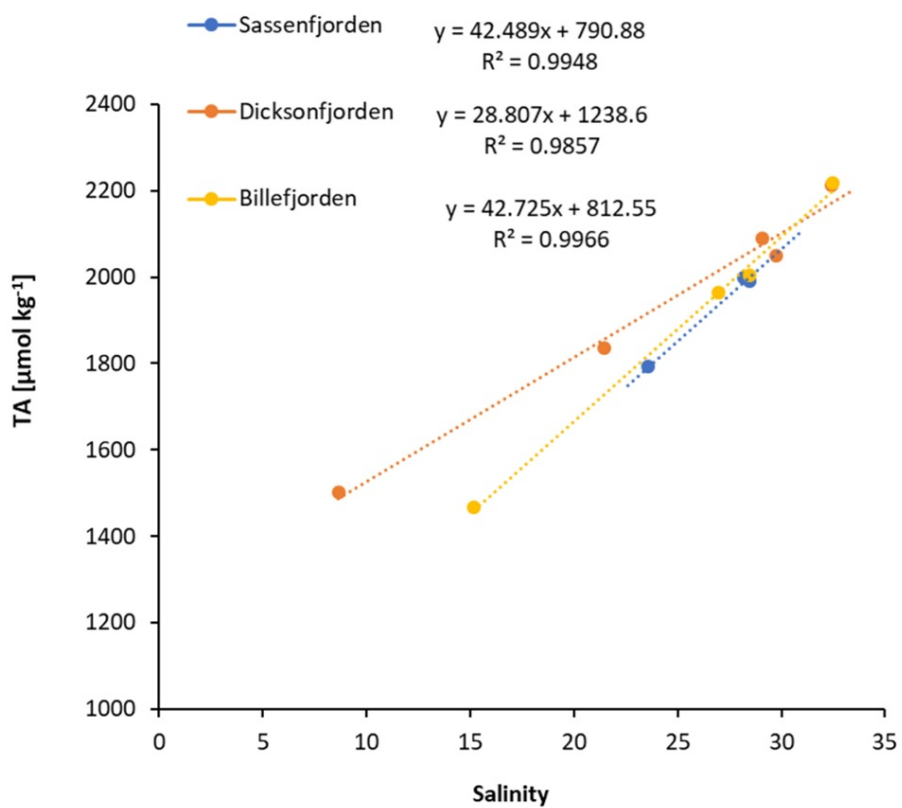


Figure 7. Linear correlation between salinity and TA collected using the carbonate profiler in the high-Arctic fjords of Sassenfjorden, Dicksonfjorden, and Billefjorden.

et al. (2021b), suggesting that the TA freshwater end member varies here in an even broader range than expected. This finding was possible thanks to the application of the carbonate profiler, which allowed for a precise sampling of the surface water layer (where the freshwater spreads) for carbonate system parameters, including TA. Although this result was achieved during operability tests of the carbonate profiler, it is an important contribution towards understanding the role of TA input from continental rivers (the Vistula River is the largest one) in mitigating Ocean Acidification in the Baltic Sea. At the same time, this very high freshwater TA end member (reported in this study for the first time for this region) indicates the need for further research in this area towards better resolving TA loads from the southern Baltic Sea catchment, which is in turn necessary to understand the alkalinity budget in the Baltic (Kuliński et al., 2022). All this demonstrates the utility of the carbonate profiler in resolving complex biogeochemical profiles in stratified waters and in obtaining accurate estimations of freshwater end-member properties by performing only a vertical profile in the vicinity of the estuaries.

3.2.2 Test 2: The turbid plumes of the Arctic fjords

The results from pCO_2 , TA, DIC, pH, temperature, and salinity measurements at the three profiles collected within the turbid plumes in the fjord waters are presented in Figure 6. The sampling covered the first 20 meters of the water column in all the locations. The largest biogeochemical gradients, as reflected in all the measured parameters, were recorded in the surface water layer and were clearly related to the water freshening (see Figure 6). The measured salinity varied significantly across all profiles (ranging from 8.66 to 33.31), increasing from the surface to the deeper waters. Out of this range, most of the variability (79% in the Dicksonfjorden profile, 74% in Billefjorden, and 71% in Sassenfjorden) occurred in the upper 5 m of the water column. Along with salinity changes, TA, DIC, pCO_2 , and pH also exhibited the strongest variation in the uppermost layer. However, in contrast to the Vistula River plume, the freshwater inflow to the fjords diluted the seawater with respect to DIC and TA, which had a pronounced effect on decreasing surface pH, thus enhancing Ocean Acidification in the region.

The abrupt gradients measured in the surface layer of the water column with the vertical variance of TA, DIC, pH, and pCO_2 of up to $588 \mu\text{mol kg}^{-1}$, $416 \mu\text{mol kg}^{-1}$, 0.34, and $44 \mu\text{atm}$, respectively, result from the outflow of turbid water plumes formed in the land-ocean transitional zone (Meslard et al., 2018; Szeligowska et al., 2020). These turbid water plumes usually cover only the first meters of the water column, creating steep biogeochemical gradients that the carbonate profiler has successfully recorded. This seemingly simple task would be unapproachable when using other sampling methods, such as a bathometer. In fact, if we were to collect water from 1 m depth using a 1 m

long bathometer, we would collect water from a depth between 0.5 m and 1.5 m. Considering the variability identified in Dicksonfjorden (Figure 6), the water inside the bathometer would have a pH range of 7.51 at the top to 7.74 at the bottom. Thus, measured pH (and any other parameter) would vary significantly depending on the water subsample within the bathometer volume. In contrast, the carbonate profiler offers a straightforward tool for investigating steep biogeochemical gradients by collecting water samples and measuring in situ parameters (e.g., salinity, temperature, turbidity, fluorescence) with a significantly higher vertical resolution. For example, in this exercise, a resolution of 0.5 m was easily achieved.

As shown already for the Vistula River plume (section 5.2.1), it is possible to use the vertical variability of TA and salinity to estimate the TA concentration in freshwater end members with great accuracy. In Spitsbergen fjords, the relationships between TA and salinity revealed different freshwater TA in different fjords, namely $791 \mu\text{mol kg}^{-1}$ in Sassenfjorden, $813 \mu\text{mol kg}^{-1}$ in Billefjorden, and $1239 \mu\text{mol kg}^{-1}$ in Dicksonfjorden (Figure 7). These concentrations fall within the range of previously reported values for Svalbard fjords, which range from 232 to $1412 \mu\text{mol kg}^{-1}$ (Ericson et al., 2018; Fransson et al., 2015; Koziorowska-Makuch et al., 2023). All this data, including this study, proves that continental runoff in Arctic fjords reduces the TA in surface waters and thus lowers its capacity to absorb atmospheric CO_2 and enhances Ocean Acidification.

Moreover, the measured pCO_2 in surface waters (Figure 6) was higher in Dicksonfjorden ($360 \mu\text{atm}$) and Billefjorden ($314 \mu\text{atm}$) than in the deeper water layer (approx. $303 \mu\text{atm}$), but in Sassenfjorden, the surface pCO_2 was lower ($284 \mu\text{atm}$). These significant changes may be attributed to the different freshwater sources that influence the fjords. While Dicksonfjorden and Billefjorden are both heavily glaciated catchments, Sassenfjorden is primarily influenced by Sassenelva, a river that drains a permafrost-rich valley (McGovern et al., 2020). Overall, the carbonate profiler allowed us to highlight the complex stratification patterns in the Arctic fjords, which have a direct impact on biogeochemical changes and the structure of the marine carbonate system. Moreover, the data show that continental runoff in the Svalbard archipelago enhances ocean acidification in coastal areas, where its surface waters have a lower capacity to uptake atmospheric CO_2 .

4. Conclusion

In this study, we designed a low-cost and easy-to-set-up upper water column sampler that can be easily incorporated into measurement systems on research vessels (and beyond). Combined with the ship's CTD profiler, they form a PUMP-CTD system that can be easily deployed on a variety of vessels regardless of their size and technical sophistication. Just by switching the water source to this PUMP-CTD, it can be used to feed the commonly used systems for

equilibrator-based continuous pCO₂ measurements (typically using the ship's pumping system having the water inlet at a fixed depth between 2 and 10 m) and extend their applicability also towards the water column sampling, including the precise sampling of the surface water layer. This is of great importance for accurately measuring seawater pCO₂ at the surface in stratified coastal water bodies (having often strong vertical biogeochemical gradients), which are to be used further for air/sea CO₂ flux calculations. As the water supply from the submersible pump is sufficient to be split, in addition to supplying the equilibrator-based continuous pCO₂ measurements, it also serves other receivers. The system allows for precise sampling of the full set of marine carbonate system parameters, namely TA, DIC, pH, and pCO₂. This feature is extremely useful in coastal waters, which, due to ion anomalies and the significant influence of non-parameterized acid-base constituents of seawater, often require a complete set of data on the structure of the marine carbonate system – a requirement that is considered excessive in open ocean waters.

The test performed in the open waters of the Greenland Sea shows that the system was able to obtain rapid and more accurate pCO₂ measurements in the water column than any other commercial method. Measurements of pCO₂ in the estuarine system of the Baltic Sea and the Spitsbergen fjords show that measurements using the carbonate profiler can be utilized as an easy tool to obtain the vertical distribution of pCO₂, including near-surface results, and thus improve estimations of air-sea CO₂ fluxes in stratified regions. The profiles also demonstrate an excellent capacity to obtain, in parallel with the continuous pCO₂ measurements, automated or discrete pH measurements and discrete samples for TA and DIC, with excellent correlation to in situ measured parameters. We also demonstrated the carbonate profiler's applicability in obtaining accurate estimations of the freshwater end-members' properties by only performing a vertical profile in the vicinity of the estuaries. For this, we used the correlation between precisely sampled TA and in situ salinity. The results from the Baltic Sea showed not only an excellent correlation in the four profiles ($R^2 = 0.98$) but also a good reproducibility, i.e., the freshwater TA of $4069 \mu\text{mol kg}^{-1}$ estimated with the variation of only $\pm 12 \mu\text{mol kg}^{-1}$ (less than 1% of the estimated value). These TA results confirm the important role of the Vistula River as a net source of TA for the Baltic and reveal very high TA concentrations in the Vistula River that have not been reported before for this region. A similar utility of the carbonate profiler has been observed for the Spitsbergen fjords. However, the estimated TA freshwater end members were much lower and highly variable between the individual fjords (ranging from 790 to $1240 \mu\text{mol kg}^{-1}$). Still, all of them demonstrated that the continental runoff in the Svalbard archipelago lowers the buffer capacity of the seawater, reduces its potential to uptake

atmospheric CO₂, and enhances Ocean Acidification. To sum up, the carbonate profiler we designed represents an easy-to-implement and low-cost tool allowing the scientific community to obtain state-of-the-art measurements of all the marine carbonate parameters with a vertical resolution better than 0.5 meters, and providing new possibilities for observations and quantifications of ocean acidification, carbon inventory, and air-sea CO₂ fluxes in highly stratified environments.

Data availability

The data presented in this study are publicly available in the online data repositories of GeoNetwork (Aguado Gonzalo et al., 2025b; <https://doi.org/10.48457/IOPAN.2025.515>).

Funding sources

The author(s) declare that financial support was received for the research, authorship, and/or publication of this article. The study was conducted within the framework of Grant No. 2019/34/E/ST10/00167 (Arctic data), 2021/41/B/ST10/00946 (Baltic Sea pCO₂ data), and 2023/49/B/ST10/02690 (TA, DIC, and pH data); all three of them financed by the Polish National Science Centre. The interpretation of the results in terms of their contextualization was supported by the European Union's Horizon Europe research and innovation programme under Grant Agreement No. 101136480 (SEA-Quester).

Authors contribution

Author contributions: CRediT FG: Conceptualization, Methodology, Writing – review & editing, Data curation, Formal analysis, Investigation, Methodology, Visualization, Writing – original draft. KKo: Data curation, Writing – review & editing. LB: Data curation. AL: Writing – review & editing. KKu: Conceptualization, Methodology, Funding acquisition, Project administration, Supervision, Validation, Writing – review & editing.

Acknowledgments

We would like to thank the captain and crew of the r/v *Oceania* for their enthusiasm and support throughout the sampling process, as well as the manuscript reviewers for their valuable comments.

Conflict of interest

None declared.

References

Aguado Gonzalo, F., Koziorowska, K., Szymczyska, B., Kuliński, K., 2025. *The Consistency between Calculated*

731 and Measured Variables of the Marine Carbonate Sys- 786
 732 tem in Arctic Open and Coastal Waters. Mar. Chem. 787
 733 (pre-print). 788
 734 <https://doi.org/10.2139/ssrn.5205880> 789
 735 Aguado Gonzalo, F., Koziorowska, K., Bromboszcz-Szczy- 790
 736 pior, L., Kulinski, K., 2025b. High resolution, vertical 791
 737 distribution of the marine carbonate system in estuar- 792
 738 ine waters of the Baltic Sea and Arctic fjords (Svalbard 793
 739 Archipelago). [Dataset]. Geonetwork. 794
 740 <https://doi.org/10.48457/IOPAN.2025.515> 795
 741 Aguado Gonzalo, F., Stokowski, M., Koziorowska-Makuch, 796
 742 K., Makuch, P., Beszczyńska-Möller, A., Kukliński, P., 797
 743 Kukliński, K., 2024. Key processes controlling the vari- 798
 744 ability of the summer marine CO₂ system in Fram Strait 799
 745 surface waters. Front. Mar. Sci. 11, 1–19. 800
 746 <https://doi.org/10.3389/fmars.2024.1464653> 801
 747 Ahmed, M.M.M., Else, B.G.T., Capelle, D., Miller, L.A., Pa- 802
 748 pakyriakou, T., 2020. Underestimation of surface pCO₂ 803
 749 and air-sea CO₂ fluxes due to freshwater stratification 804
 750 in an Arctic shelf sea, Hudson Bay. Elementa 8. 805
 751 <https://doi.org/10.1525/elementa.084> 806
 752 Arruda, R., Atamanchuk, D., Cronin, M., Steinhoff, T., Wal- 807
 753 lence, D.W.R., 2020. At-sea intercomparison of three un- 808
 754 derway pCO₂ systems. Limnol. Oceanogr. Methods 18, 809
 755 63–76. 810
 756 <https://doi.org/10.1002/lom3.10346> 811
 757 Azevedo, C.C., González-Dávila, M., Santana-Casiano, J.M., 812
 758 González-Santana, D., Caldeira, R.M.A., 2024. Impact 813
 759 of sampling depth on CO₂ flux estimates. Sci. Rep. 14, 814
 760 1–9. 815
 761 <https://doi.org/10.1038/s41598-024-69177-x> 816
 762 Bauer, J.E., Cai, W.J., Raymond, P.A., Bianchi, T.S., Hopkinson, 817
 763 C.S., Regnier, P.A.G., 2013. The changing carbon cycle 818
 764 of the coastal ocean. Nature 504, 61–70. 819
 765 <https://doi.org/10.1038/nature12857> 820
 766 Bresnahan, P.J., Martz, T.R., Takeshita, Y., Johnson, K.S., 821
 767 LaShomb, M., 2014. Best practices for autonomous 822
 768 measurement of seawater pH with the Honeywell Du- 823
 769 rafet. Methods Oceanogr. 9, 44–60. 824
 770 <https://doi.org/10.1016/j.mio.2014.08.003> 825
 771 Cai, W.J., 2011. Estuarine and coastal ocean carbon paradox: 826
 772 CO₂ sinks or sites of terrestrial carbon incineration? 827
 773 Ann. Rev. Mar. Sci. 3, 123–145. 828
 774 <https://doi.org/10.1146/annurev-marine-120709-142723> 829
 775 Carter, B.R., Radich, J.A., Doyle, H.L., Dickson, A.G., 2013. An 830
 776 automated system for spectrophotometric seawater pH 831
 777 measurements. Limnol. Oceanogr. Methods 11, 16–27. 832
 778 <https://doi.org/10.4319/lom.2013.11.16> 833
 779 Carter, B.R., Sharp, J.D., García-ib, M.I., Woosley, R.J., Fong, 834
 780 M.B., Alvarez, M., Barbero, L., Clegg, S.L., Easley, R., 835
 781 Fassbender, A.J., Li, X., Schockman, K.M., Wang, Z.A., 2024., 836
 782 Review Random and systematic uncertainty in 837
 783 ship-based seawater carbonate chemistry observations, 838
 784 1–16. 839
 785 <https://doi.org/10.1002/lno.12674> 840
 786 Chen, B., Cai, W.J., Chen, L., 2015. The marine carbonate 787
 787 system of the Arctic Ocean: Assessment of internal con- 788
 788 sistency and sampling considerations, summer 2010. 789
 789 Mar. Chem. 176, 174–188. 790
 790 <https://doi.org/10.1016/j.marchem.2015.09.007> 791
 791 Clarke, J.S., Achterberg, E.P., Connelly, D.P., Schuster, U., 792
 792 Mowlem, M., 2017. Developments in marine pCO₂ mea- 793
 793 surement technology; towards sustained *in situ* obser- 794
 794 vations. TrAC – Trends Anal. Chem. 88, 53–61. 795
 795 <https://doi.org/10.1016/j.trac.2016.12.008> 796
 796 Clayton, T.D., Byrne, R.H., 1993. Spectrophotometric seawa- 797
 797 ter pH measurements: total hydrogen ion concentration 798
 798 scale calibration of m-cresol purple and at-sea results. 799
 799 Deep. Res. Pt. I 40, 2115–2129. 800
 800 [https://doi.org/10.1016/0967-0637\(93\)90048-8](https://doi.org/10.1016/0967-0637(93)90048-8) 801
 801 Cross, J.N., Mathis, J.T., Pickart, R.S., Bates, N.R., 2018. For- 802
 802 mation and transport of corrosive water in the Pacific 803
 803 Arctic region. Deep. Res. Pt. II Top. Stud. Oceanogr. 804
 804 152, 67–81. 805
 805 <https://doi.org/10.1016/j.dsr2.2018.05.020> 806
 806 Dai, M., Su, J., Zhao, Y., Hofmann, E.E., Cao, Z., Cai, W.J., Gan, 807
 807 J., Lacroix, F., Laruelle, G.G., Meng, F., Mudieller, J.D., 808
 808 Regnier, P.A.G., Wang, G., Wang, Z., 2022. Carbon Fluxes 809
 809 in the Coastal Ocean: Synthesis, Boundary Processes, 810
 810 and Future Trends. Annu. Rev. Earth Planet. Sci. 50, 811
 811 593–626. 812
 812 <https://doi.org/10.1146/annurev-earth-032320-090746> 813
 813 Dickson, A.G.; Sabine, C.L. and Christian, J.R., 2007. Guide 814
 814 to best practices for ocean CO₂ measurement. Sidney, 815
 815 British Columbia, North Pacific Marine Science Orga- 816
 816 nization, 191 pp. (PICES Special Publication 3; IOCOP 817
 817 Report 8). 818
 818 <https://doi.org/10.25607/OPB-1342> 819
 819 Dickson, A.G., 1981. An exact definition of total alkalinity 820
 820 and a procedure for the estimation of alkalinity and 821
 821 total inorganic carbon from titration data. Deep Sea 822
 822 Res. Pt. A, Oceanogr. Res. Pap. 28, 609–623. 823
 823 [https://doi.org/10.1016/0198-0149\(81\)90121-7](https://doi.org/10.1016/0198-0149(81)90121-7) 824
 824 Dickson, A.G., Afghan, J.D., Anderson, G.C., 2003. Reference 825
 825 materials for oceanic CO₂ analysis: A method for the cer- 826
 826 tification of total alkalinity. Mar. Chem. 80, 185–197. 827
 827 [https://doi.org/10.1016/S0304-4203\(02\)00133-0](https://doi.org/10.1016/S0304-4203(02)00133-0) 828
 828 Dickson, A.G., Wesolowski, D.J., Palmer, D.A., Mesmer, R.E., 829
 829 1990. Dissociation constant of bisulfate ion in aqueous 830
 830 sodium chloride solutions to 250°C. J. Phys. Chem. 94, 831
 831 7978–7985. 832
 832 <https://doi.org/10.1021/j100383a042> 833
 833 Ericson, Y., Falck, E., Chierici, M., Fransson, A., Kristiansen, 834
 834 S., Platt, S.M., Hermansen, O., Myhre, C.L., 2018. Tem- 835
 835 poral Variability in Surface Water pCO₂ in Adventfjorden 836
 836 (West Spitsbergen) With Emphasis on Physical and Bio- 837
 837 geochemical Drivers. J. Geophys. Res. Ocean. 123, 838
 838 4888–4905. 839
 839

841 <https://doi.org/10.1029/2018JC014073> 896

842 Fietzek, P., Fiedler, B., Steinhoff, T., Körtzinger, A., 2014. 897
In situ quality assessment of a novel underwater pCO 898
2 sensor based on membrane equilibration and NDIR 899
spectrometry. *J. Atmos. Ocean. Technol.* 31, 181–196. 900
<https://doi.org/10.1175/JTECH-D-13-00083.1> 901

843 Fransson, A., Chierici, M., Nomura, D., Granskog, M.A., Kris- 902
tiansen, S., Martma, T., Nehrke, G., 2015. *Effect of* 903
glacial drainage water on the CO₂ system and ocean 904
acidification state in an Arctic tidewater-glacier fjord 905
during two contrasting years. *J. Geophys. Res. Ocean.* 906
<https://doi.org/10.1002/2014JC010320> 907

844 Friedlingstein, P., O'Sullivan, M., Jones, M.W., Andrew, R.M., 908
Hauck, J., Landschützer, P., Le Quéré, C., Li, H., Luijkx, 909
I.T., Olsen, A., Peters, G.P., 2025. *Global carbon budget* 910
Earth Syst. Sci. Data 17, 965–1039. 911
<https://doi.org/10.5194/essd-17-965-2025> 912

845 Humphreys, M. P. and Matthews, R. S. 2024. *Calkulate: total* 913
alkalinity from titration data in Python. Zenodo. 914
<https://doi.org/10.5281/zenodo.2634304> 915

846 Jiang, Z.P., Hydes, D.J., Hartman, S.E., Hartman, M.C., Camp- 916
bell, J.M., Johnson, B.D., Schofield, B., Turk, D., Wallace, 917
D., Burt, W.J., Thomas, H., Cosca, C., Feely, R., 2014. *Ap- 918
plication and assessment of a membrane-based pCO₂* 919
sensor under field and laboratory conditions. *Limnol.* 920
Oceanogr. Methods 12, 264–280. 921
<https://doi.org/10.4319/lom.2014.12.264> 922

847 Johengen, T., Smith, G.J., Schar, D., Atkinson, M., Purcell, H., 923
Loewenstein, D., Epperson, Z., Tamburri, M., 2015. *Performance* 924
Verification Statement for the Sunburst 925
SAMI-pH Sensor. Solomons, MD, Alliance for Coastal 926
Technologies, 63 pp. (ACTVS15-06). 927
<http://doi.org/10.25607/OPB-306> 928

848 Kerr, D.E., Turner, C., Grey, A., Keogh, J., Brown, P.J., Kelleher, 929
B.P., 2023. *OrgAlkCalc: Estimation of organic alkalinity* 930
quantities and acid-base properties with proof of concept 931
in Dublin Bay. *Mar. Chem.* 251, 104234. 932
<https://doi.org/10.1016/j.marchem.2023.104234> 933

849 Koziorowska-Makuch, K., Szymczyha, B., Thomas, H., 934
Kuliński, K., 2023. *The marine carbonate system vari- 935
ability in high meltwater season (Spitsbergen Fjords,* 936
Svalbard). *Prog. Oceanogr.* 211. 937
<https://doi.org/10.1016/j.pocean.2023.102977> 938

850 Kuliński, K., Hammer, K., Schneider, B., Schulz-Bull, D., 2016. 939
Remineralization of terrestrial dissolved organic carbon 940
in the Baltic Sea. *Mar. Chem.* 181, 10–17. 941
<https://doi.org/10.1016/j.marchem.2016.03.002> 942

851 Kuliński, K., Rehder, G., Asmala, E., Bartosova, A., 943
Carstensen, J., Gustafsson, B., Hall, P.O.J., Humborg, C., 944
Jilbert, T., Jürgens, K., Meier, H.E.M., Müller-Karulis, B., 945
Naumann, M., Olesen, J.E., Savchuk, O., Schramm, A., 946
Slomp, C.P., Sofiev, M., Sobek, A., Szymczyha, B., Unde- 947
man, E., 2022. *Biogeochemical functioning of the Baltic* 948
Sea. *Earth Syst. Dynam.* 13, 633–685. 949
<https://doi.org/10.5194/esd-13-633-2022> 950

841 Kuliński, K., Schneider, B., Szymczyha, B., Stokowski, M., 896
2017. *Structure and functioning of the acid-base system* 897
in the Baltic Sea. *Earth Syst. Dynam.* 8, 1107–1120. 898
<https://doi.org/10.5194/esd-8-1107-2017> 899

842 Lai, C.Z., DeGrandpre, M.D., Darlington, R.C., 2018. *Aut- 900
tonomous optofluidic chemical analyzers for marine ap- 901
plications: Insights from the Submersible Autonomous* 902
Moored Instruments (SAM) for pH and pCO₂. *Front.* 903
Mar. Sci. 4, 1–11. 904
<https://doi.org/10.3389/fmars.2017.00438> 905

843 Lee, K., Kim, T.W., Byrne, R.H., Millero, F.J., Feely, R.A., Liu, 906
Y.M., 2010. *The universal ratio of boron to chlorinity for* 907
the North Pacific and North Atlantic oceans. *Geochim.* 908
Cosmochim. Acta 74, 1801–1811. 909
<https://doi.org/10.1016/j.gca.2009.12.027> 910

844 Lewis, E., Wallace, D., and Allison, L. J., 1998. Program 911
developed for CO₂ system calculations (TN (United 912
States: Brookhaven Natl. Lab., Dept. Appl. Sci., Upton, 913
NY; Oak Ridge Natl. Lab., Carbon Dioxide Information 914
Analysis Center). No. ORNL/CDIAC-105). 915

845 Liu, P., He, S., Wei, H., Wang, J., Sun, C., 2015. *Characteri- 916
zation of α -Fe₂O₃/ γ -Al₂O₃ catalysts for catalytic wet* 917
peroxide oxidation of m-Cresol. *Ind. Eng. Chem. Res.* 918
54, 130–136. 919
<https://doi.org/10.1021/ie5037897> 920

846 Lueker, T.J., Dickson, A.G., Keeling, C.D., 2000. *Ocean pCO₂* 921
calculated from dissolved inorganic carbon, alkalinity, 922
*and equations for K₁ and K₂: validation based on lab- 923
oratory measurements of CO₂ in gas and seawater at* 924
equilibrium. *Marine Chem.* 70(1–3), 105–119. 925

847 McGovern, M., Pavlov, A.K., Deininger, A., Granskog, M.A., 926
Leu, E., Søreide, J.E., Poste, A.E., 2020. *Terrestrial In- 927
puts Drive Seasonality in Organic Matter and Nutrient* 928
Biogeochemistry in a High Arctic Fjord System (Ilsfjord, 929
Svalbard). *Front. Mar. Sci.* 7, 1–15. 930
<https://doi.org/10.3389/fmars.2020.542563> 931

848 Meslard, F., Bourrin, F., Many, G., Kerhervé, P., 2018. *Sus- 932
pended particle dynamics and fluxes in an Arctic fjord* 933
(Kongsfjorden, Svalbard). *Estuar. Coast. Shelf Sci.* 204, 934
212–224. 935
<https://doi.org/10.1016/j.ecss.2018.02.020> 936

849 Millero, F.J., 2007. *The marine inorganic carbon cycle*. *Chem.* 937
Rev. 107, 308–341. 938
<https://doi.org/10.1021/cr0503557> 939

850 Mosley, L.M., Husheer, S.L.G., Hunter, K.A., 2004. *Spec- 940
trophotometric pH measurement in estuaries using thy- 941
mol blue and m-cresol purple*. *Mar. Chem.* 91, 175–186. 942
<https://doi.org/10.1016/j.marchem.2004.06.008> 943

851 Mosley, L.M., Liss, P.S., 2020. *Particle aggregation, pH* 944
*changes and metal behaviour during estuarine mix- 945
ing: Review and integration*. *Mar. Freshw. Res.* 71, 946
300–310. 947
<https://doi.org/10.1071/MF19195> 948

852 Orr, J.C., Epitalon, J.M., Dickson, A.G., Gattuso, J.P., 2018. 949
Routine uncertainty propagation for the marine carbon 950

951 dioxide system. *Mar. Chem.* 207, 84–107. 1006
 952 <https://doi.org/10.1016/j.marchem.2018.10.006> 1007

953 Perez, F.F., Fraga, F., 1987. *Association constant of fluo- 1008
 954 ride and hydrogen ions in seawater*. *Mar. Chem.* 21, 1009
 955 161–168. 1010
[https://doi.org/10.1016/0304-4203\(87\)90036-3](https://doi.org/10.1016/0304-4203(87)90036-3) 1011

956 Pierrot, D., Lewis, E., Wallace, D.W.R., 2006. *MS Excel Pro- 1012
 958 gram Developed for CO₂ System Calculations*. Tech. Rep. 1013
 959 Carbon Dioxide Inf. Anal. Cent. Oak Ridge Natl. Lab., 1014
 960 U.S. DOE, Oak Ridge, Tenn. 1015
<https://doi.org/10.1016/s41586-021-04339-9> 1016

961 Regnier, P., Resplandy, L., Najjar, R.G., Caias, P., 2022. *The 1017
 962 land-to-ocean loops of the global carbon cycle*. *Nature* 1018
 963 603, 401–410. 1019
<https://doi.org/10.1038/s41586-021-04339-9>

964 Resplandy, L., Keeling, R.F., Rödenbeck, C., Stephens, B.B., 1013
 965 Khatiwala, S., Rodgers, K.B., Long, M.C., Bopp, L., Tans, 1014
 966 P.P., 2018. *Revision of global carbon fluxes based on 1015
 968 a reassessment of oceanic and riverine carbon transport*. 1016
 969 *Nat. Geosci.* 11, 504–509. 1017
<https://doi.org/10.1038/s41561-018-0151-3> 1018

970 Schar, D., Atkinson, M., Johengen, T., Pinchuk, A., Purcell, H., 1018
 971 Robertson, C., Smith, G.J., 2010a. *Pro-Oceanus Systems 1019
 973 Inc. PSI CO₂-Pro TM*. Situ 1–24.

974 Schar, D., Atkinson, M., Johengen, T., Pinchuk, A., Purcell, H., 1013
 975 Robertson, C., Smith, G.J., Tamburri, M., 2010b. *Per- 1014
 976 formance Demonstration Statement Sunburst Sensors 1015
 977 SAMI-CO sub(2)*. ACT Technol. Eval. Reports DS10-04, 1016
 978 1–23.

979 Signori, R.T., de Souza, S.A., Ferreira, R.B., da Silva, J.T., de 1017
 980 Andrade, A.M.D., dos Reis, G.C.G., 2021. *Data acquisition 1018
 981 and transmission system for carbon dioxide analysis*. 1019
 982 *Rev. Bras. Meteorol.* 36, 115–123.
<https://doi.org/10.1590/0102-77863610003>

983 Stokowski, M., Makuch, P., Rutkowski, K., Wichorowski, M., 1013
 984 Kuliński, K., 2021a. *A system for the determination of 1014
 985 surface water pCO₂ in a highly variable environment, 1015
 986 exemplified in the southern Baltic Sea*. *Oceanologia* 1016
 987 63(2), 276–282.
<https://doi.org/10.1016/j.oceano.2021.01.001> 1017

988 Stokowski, M., Winogradow, A., Szymczycha, B., Carstensen, 1018
 989 J., Kuliński, K., 2021b. *The CO₂ system dynamics in the 1019
 990 vicinity of the Vistula River mouth (the southern Baltic 1013
 991 Sea): A baseline investigation*. *Estuar. Coast. Shelf Sci.* 1014
 992 258, 2–11.
<https://doi.org/10.1016/j.ecss.2021.107444> 1015

993 Strady, E., Pohl, C., Yakushev, E. V., Krüger, S., Hennings, U., 1016
 994 2008. *PUMP-CTD-System for trace metal sampling with 1017
 995 a high vertical resolution. A test in the Gotland Basin, 1018
 996 Baltic Sea*. *Chemosphere* 70, 1309–1319.
<https://doi.org/10.1016/j.chemosphere.2007.07.051> 1019

997 Szeligowska, M., Trudnowska, E., Boehnke, R., Dąbrowska, 1013
 998 A.M., Wiktor, J.M., Sagan, S., Błachowiak-Samołyk, K., 1014
 999 2020. *Spatial Patterns of Particles and Plankton in the 1015
 1000 Warming Arctic Fjord (Isfjorden, West Spitsbergen) in 1016
 1001 Seven Consecutive Mid-Summers (2013–2019)*. *Front.* 1017

1002
 1003
 1004
 1005

Mar. Sci. 7, 1–18.
<https://doi.org/10.3389/fmars.2020.00584>

Takahashi, T., Olafsson, J., Goddard, J.G., Chipman, D.W., 1006
 Sutherland, S.C., 1993. *Seasonal variation of CO₂ and 1007
 1008 nutrients in the high-latitude oceans: A comparative 1009
 1009 study*. *Global Biogeochem. Cycles* 7, 843–878.
 1010

Ulfsbo, A., Kuliński, K., Anderson, L.G., Turner, D.R., 2015. 1011
 1012 *Modelling organic alkalinity in the Baltic Sea using 1013
 1013 a Humic-Pitzer approach*. *Mar. Chem.* 168, 18–26.
<https://doi.org/10.1016/j.marchem.2014.10.013>
 1014

Woosley, R.J., Millero, F.J., Takahashi, T., 2017. *Internal 1015
 1016 consistency of the inorganic carbon system in the Arctic 1017
 1017 Ocean*. *Limnol. Oceanogr. Methods* 15, 887–896.
<https://doi.org/10.1002/lom3.10208>
 1018

1019